GLAND SEGMENTATION GUIDED BY GLANDULAR STRUCTURES: A LEVEL SET FRAMEWORK WITH TWO LEVELS

Chen Wang

University of Electronic Science and Technology of China

Ji Bao, Hong Bu

Sichuan University

ABSTRACT

Pathologic diagnosis is the gold standard of clinical diagnosis. The identification and segmentation of histological structures are the prerequisites to disease diagnosis. In clinic, doctors often suffer from time consuming and the disagreements from different doctors about observation results. Hence, an automatic precise segmentation method is important for auxiliary diagnosis. We propose a level set framework using 0,k level set representing the boundary of lumen regions and epithelial layers for gland segmentation. The validation has been performed on clinical data of West China Hospital, Sichuan University. The experiment results show that our method has a better performance and is robust to the shape variety of endometrial glands.

Index Terms— gland segmentation, level set, endometrial gland

1. INTRODUCTION

Pathologic diagnosis is the gold standard of clinical diagnosis. The identification of certain histological structures such as cancer nuclei or glands is the prerequisite to disease diagnosis in pathology [1]. With the development of digital pathology, the segmentation of the pathologic structures based on whole slice image(WSI) has become popular in recent years. As one feature in pathologic diagnosis, morphology of glands plays an important role. For example, in endometrial gland hematoxylin & eosin (H&E) stained images, the ratio of the gland area to the stromal nuclei area is a leading feature for simple endometrial hyperplasias diagnosis in clinic (As the Fig. 1(a) shows, a gland H&E stained image mainly consists of gland, stromal nuclei, vessels and also erythrocytic in specific regions). Thus, the precise segmentation of glands in H&E stained image is clinically significant.

As shown in Fig. 1(b), the endometrial gland contains two structures, which are lumens (the inner regions in white) and epithelial layers (nuclear periphery). In clinic, the segmentation is done by manual identification in the optical microscopic images of H&E stained slides. However, the manual identification is time consuming. And different doctors sometimes obtain the different clinical results due to the following three factors: 1.shape variety of glands(Fig.2); 2.different staining degree of two H&E stained images; 3.numerous glands in an image. Thus, an automated segmentation algorithm is needed for auxiliary diagnosis.

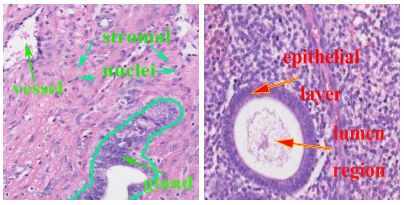

(a) major structures (b) glandular structures

Fig. 1. illustration of the morphology of glands in H&E stained image

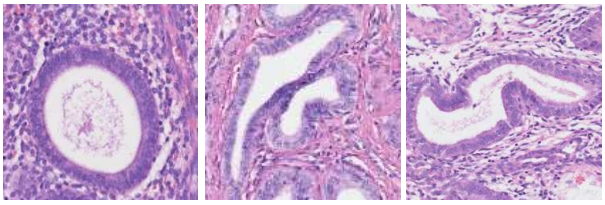

Fig. 2. shape variety of endometrial glands

A popular scheme for gland segmentation is a combination of classification and level set method, which consist of three stages [1]. First a classifier is trained to recognize nuclear, then structural constraints are used to reduce the number of false positive regions. Finally, a level set under the control of the Bayesian probability scene is initialized and evolved. For example, Naik et al. [2] proposed a gland segmentation method in this scheme incorporated to template approaches. However, this scheme needs two level sets to segment lumen region and nuclear periphery, respectively. Besides, Cigdem et al. [3] proposed an object-graph approach. By modeling the regular structure of glands, it achieves reliable results on circular glands. However, the method can't deal with the shape variety of glands. Recently, the popular deep learning methods are also applied in gland segmentation. Chen et al. [4] proposed an efficient deep contour-aware net-

work (DCAN) under a unified multi-task learning framework. Although deep learning methods can obtain reliable results, it requires numerous training data and training time, and possibly achieves declined performance when applying to a varied object which is not similar to the training data.

In our proposed method, the segmentation process is finished on a level set framework which only one level set is used. Considered the glandular structures(lumens and epithelial layers), we use the zero level set to represent the boundary of the lumen regions and the k-level set to represent the boundary of the epithelial layers. The initial level set can be obtained by k-means algorithm and the evolution of level set is driven only by the intensity of R,G,B channels.

2. METHOD

2.1. Preprocessing

The original H&E stained image data are high-resolution images, which brings the segmentation two major difficulties: High-resolution images are stored in a large matrix, which violently slows the speed of the evolution of the level set since the computation on large data is time consuming. Besides, the segmentation algorithm on high-resolution images will obtain detailed structures such as nuclei, hence fail to obtain the boundary of epithelial layers. In order to deal with these two difficulties, we employ down sampling and smoothing to the original images. Our goal is to decrease the size of data and weaken the details, which makes the computation less time consuming and the evolution not influenced by nuclei. The original images are down sampled as 1/8, and a smoothing process is performed before down sampling.

2.2. Level set framework for gland segmentation

In our method, gland segmentation is achieved by looking for a level set function which minimizes the energy functional which consists of two major terms: data term and regularization term. The energy functional is defined as follows:

$$E(\phi) = \mu R_p(\phi) + \lambda L_g(\phi) + \alpha A_g(\phi) \tag{1}$$

where $R_p(\phi)$ is the distance regularization term which keeps the regularity of level set; $L_g(\phi)$ and $A_g(\phi)$ are data terms which can be defined differently in terms of specific applications. μ, λ and α are the coefficients of the corresponding energies.

For segmentation of the lumen region, we use the original DRLSE model [5]. The level set is driven by the energy functional as formula (1) with each energy functional term defined as follows:

$$R_p(\phi) = \int_\Omega p(|\nabla\phi|)dx \tag{2}$$

$$L_g(\phi) = \int_\Omega g\delta(\phi)|\nabla\phi|dx \tag{3}$$

$$A_g(\phi) = \int_\Omega gH(-\phi)dx \tag{4}$$

where p is a potential function $p : [0, +\infty) \to R$ which can be defined as $p(s) = \frac{1}{2}(s-1)^2$, and H, δ are the Heaviside function and Dirac function, respectively. And g is edge indicator function defined as:

$$g = \frac{1}{1 + |\nabla G_\sigma * I|^2} \tag{5}$$

where G_σ is Gaussian kernel with a standard deviation σ. With the edge indicator function g, $L_g(\phi)$ plays a role to drive the contour towards the boundary with higher gradient value. And weighted area term $A_g(\phi)$ plays a role in accelarating the evolution of the contours.

Through representing the contour of the epithelial layer by the k-level of the same level set, we change the original DRLSE model to two levels (i.e. 0,k level) to segment these desired regions. Similar to the segmentation of lumen regions which drives the 0-level set only, we use 0,k-level set simultaneously to represent the lumen regions and epithelial layers. The corresponding energy functional is (1) with the following terms:

$$L_g(\phi) = \int_\Omega g[\lambda_1\delta(\phi) + \lambda_2\delta(\phi - k)]|\nabla\phi|dx \tag{6}$$

$$A_g(\phi) = \alpha_0 \int_\Omega gH(-\phi)dx + \alpha_k \int_\Omega gH(-\phi + k)dx \tag{7}$$

where λ_1,λ_2,α_0 and α_k are coefficients respectively. $R_p(\phi)$ is the same as formula (2). Here, $L_g(\phi)$ and $A_g(\phi)$ play the similar role as in formula (3)(4) while here drive both 0,k-level set to the desired boundaries.

The desired boundaries which represented by the 0,k-level set are obtained by looking for a level set function which minimizes the energy functional. Thus, we propose to minimize the energy functional. According to calculus of variations [6], we minimize the energy functional $E(\phi)$ by finding the steady state solution of the gradient flow equation:

$$\frac{\partial\phi}{\partial t} = -\frac{\partial E}{\partial\phi} \tag{8}$$

where $\frac{\partial E}{\partial\phi}$ is the Gâteaux derivative of the functional E. This is an evolution equation which indicates the level set to evolve towards the opposite direction of the Gâteaux derivative(i.e. the gradient descent direction). By calculating the Gâteaux derivative of energy functional (1), we can obtain the evolution equation as follows:

$$\begin{aligned}\frac{\partial\phi}{\partial t} = \mu \left[\nabla^2\phi - div\left(\frac{\nabla\phi}{|\nabla\phi|}\right) \right] \\ + \lambda\delta_\epsilon(\phi) div\left(g\frac{\nabla\phi}{|\nabla\phi|}\right) + \alpha g\delta_\epsilon(\phi)\end{aligned} \tag{9}$$

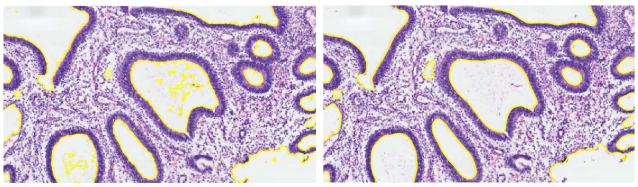

(a) Initial contour (b) Final contour of 0-level set

Fig. 3. First step: segmentation of the lumen region

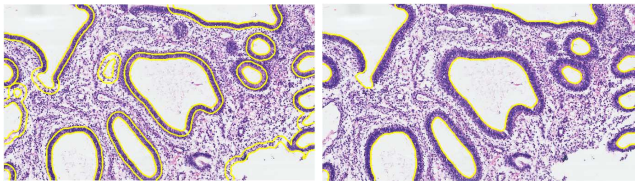

(a) Surrounding regions (b) contour after removing vessel

Fig. 4. Second step: removing vessel

$$\frac{\partial \phi}{\partial t} = \mu \left[\nabla^2 \phi - div\left(\frac{\nabla \phi}{|\nabla \phi|}\right) \right] + \alpha_0 g \delta_\epsilon(\phi) + \alpha_k g \delta_\epsilon(\phi - k) + [\lambda_1 \delta_\epsilon(\phi) + \lambda_2 \delta_\epsilon(\phi - k)] div\left(g \frac{\nabla \phi}{|\nabla \phi|}\right) \tag{10}$$

where ∇^2 represents Laplacian operator, and $div(\cdot)$ is the divergence operator. Formula (9) and (10) are the evolution equations used in the first and final step, respectively. The evolution of level set starts from the initial level set $\phi_0(x)$.

2.3. Morphology guideness: glandular structures

Although shape variety of glands and various staining degree of H&E stained images make gland segmentation a tough problem, glandular structures keeps the same, which the lumen regions are surrounded by the epithelial layer. Besides, the lumen regions are always white or mostly white regardless of the staining degree of the H&E stained image. According to the above pathology knowledge, we perform the gland segmentation process in the following three steps.

In the first step, the lumen regions are located by the zero level set. As described in section 2.2, we use the DRLSE model to segment the lumen regions. Since the lumen regions are always white or mostly white, the segmentation process can be achieved well in which the initialization of the level set can be done by simple thresholding or clustering algorithm. In our method, the initial contour is obtained by k-means algorithm, as shown in Fig. 3(a).

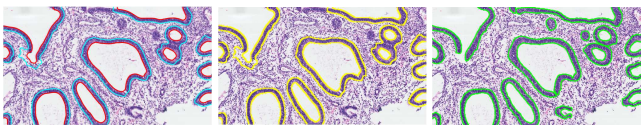

(a) 0-k level set. red: 0-level set, cyan: k-level set (b) final contour: region between 0-k level set (c) ground truth

Fig. 5. Final step: segmentation of the epithelial layer

As the Fig. 3(b) shows, in the first step our method obtained the contours of the lumen regions and vessels. In order to avoid the interference of the vessels, the second step in our method is removing the vessel regions. The morphological difference between glands and vessels is that the glands have the epithelial layers while the vessels don't. Observed that, we calculate the ratio of nuclei in the surrounding regions(as shown in Fig. 4(a)) outside the contour obtained in the first step one by one, and the region with a high ratio will be recognized as the gland region and preserved. The result after removing vessels is shown in Fig.4(b).

In the final step, the evolved level set in the first and second step is used as the initial level set. The lumen regions are still represented by the zero level of the evolved level set, while we use the k-level of the previous level set to capture the boundary of the epithelial layers. As the foregoing statement, the evolution of contours are guided by the evolution equation (10). The 0,k level set, the final contour of our method and the ground truth are shown in Fig.5.

3. EXPERIMENTS & RESULTS

3.1. Dataset and Performance measure

We use the clinical data from West China Hospital,Sichuan University for our experiments. The dataset contains 18 H&E stained images of normal or simple endometrial hyperplasia endometrial glands. Each image has a corresponding ground truth drawn by experts of West China Hospital,Sichuan University.

We use Euler Distance (ED) between obtained contours and ground truth to validate the segmentation accuracy of our proposed method. Given the contour c_s which obtained by the segmentation method and c_g which is the contour of the ground truth, ED calculates the distance from c_s to c_g.

$$ED(c_s, c_g) = \frac{1}{2}\left(\sum_{i \in c_s} D(i, c_g) + \sum_{j \in c_g} D(c_s, j)\right) \tag{11}$$

where $D(i, c_g)$ represents the distance from the pixel i to the contour c_g, which is calculated as $D(i, c_g) = \min_{j \in c_g} d(i, j)$ and $D(c_s, j)$ is defined similarly. ED is more convenient to be used for evaluating the method which only obtains the contours. Since the contour may not be closed, it is difficult to obtain the corresponding regions and the Dice similarity coefficient (DSC) can not be calculated. Because K.Nguyen et al.nguyen2012structure used for comparison obtains only contours, we can not use DSC as a measure as the most papers

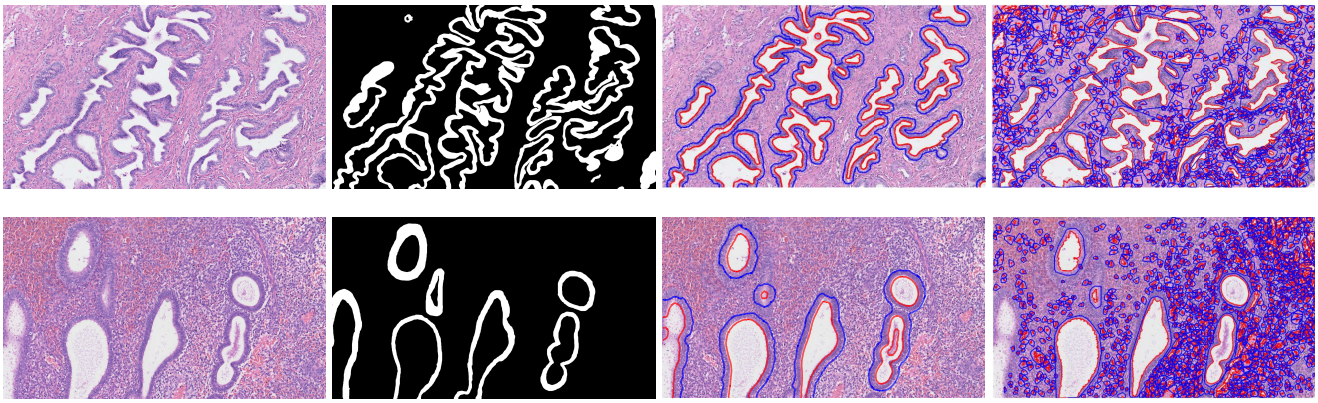

Fig. 6. Segmentation results using different methods for different shapes of endometrial glands(from left to right:original image, ground truth, our method, K.Nguyen et al.)

did. We can see that the ED will be lower if the segmentation contours are more close to the ground truth. Meanwhile, the over segmentation and the under segmentation results have a higher ED (i.e. worse performance).

3.2. Parameters

In the first step, when we apply the original DRLSE model, we set the parameters as $\triangle t = 1$, $\mu = 0.2$, and $\lambda = 5$, $\alpha = -0.3$. Since the lumen regiona are credibly segmented in the first step, we tend to evolve the k level set(representing the epithelial layer) mainly in the final step. Hence, parameters are set differently in the final step as $\alpha_0 = 0$, $\alpha_k = -1.3$, $\lambda_0 = 10$, $\lambda_k = 1$, $\triangle t = 0.5$, $\mu = 0.1$. We set $\alpha_0 = 0$ since we believe the result in the first step is reasonable and don't want to change much. And we set $\alpha_k = -1.3$ to make the k level set expanding since the initial k level set is inner the desired boundary.

3.3. Results and comparison

To validate the segmentation performance of the proposed approach, we compared with the segmentation scheme proposed in [7]. Since these two methods has different scheme, we apply these two methods on the 18 original H&E stained images for fair comparison. The down sampling process are applied only in our method and the segmentation results are put back to original size. As the Fig. 6 shows, our method is robust to the shape variety of endometrial glands. However, K.Nguyen et al. suffers from the interference of the vessel and nuclei, which obtains contours of the vessels and stromal nuclei.

The results of K.Nguyen et al. are contours only and the contours are often not closed. To compare our method with it, the ED from the contours of obtained result to ground truth is calculated, as shown in Fig. 7. The slightly worse performance of K.Nguyen et al. indicates that features extracted from one kind of gland may not suit for other glands. However, our method which only utlizes the intensities of R,G,B channels is more robust to different glandular images.

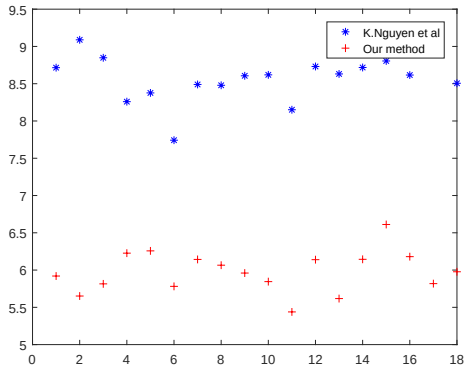

Fig. 7. ED of different methods for 18 images. The x-axis represents 18 images and the y-axis represents $log(ED)$.

4. CONCLUSION

In this paper, we proposed a level set framework with 0,k-level set for endometrial gland segmentation. For weakening the interference of nuclear and reducing time consuming, we down sample each image as $1/8$ and smooth. Compared with the majority scheme, we only utilize the intensity information of R,G,B channels and morphology structure information to construct the level set framework for segmentation. The experiments show that our method has a better performance compared with K.Nguyen et al. [7]. Our method is robust to the shape variety of glands and needs a small number of parameter changes. Hence, it can be used in clinic in the future.

5. REFERENCES

[1] Metin N Gurcan, Laura E Boucheron, Ali Can, Anant Madabhushi, Nasir M Rajpoot, and Bulent Yener,

"Histopathological image analysis: A review," *IEEE reviews in biomedical engineering*, vol. 2, pp. 147–171, 2009.

[2] Shivang Naik, Scott Doyle, Shannon Agner, Anant Madabhushi, Michael Feldman, and John Tomaszewski, "Automated gland and nuclei segmentation for grading of prostate and breast cancer histopathology," in *Biomedical Imaging: From Nano to Macro, 2008. ISBI 2008. 5th IEEE International Symposium on*. IEEE, 2008, pp. 284–287.

[3] Cigdem Gunduz-Demir, Melih Kandemir, Akif Burak Tosun, and Cenk Sokmensuer, "Automatic segmentation of colon glands using object-graphs," *Medical image analysis*, vol. 14, no. 1, pp. 1–12, 2010.

[4] Hao Chen, Xiaojuan Qi, Lequan Yu, and Pheng-Ann Heng, "Dcan: Deep contour-aware networks for accurate gland segmentation," in *Proceedings of the IEEE conference on Computer Vision and Pattern Recognition*, 2016, pp. 2487–2496.

[5] Chunming Li, Chenyang Xu, Changfeng Gui, and Martin D Fox, "Distance regularized level set evolution and its application to image segmentation," *IEEE Transactions on image processing*, vol. 19, no. 12, pp. 3243–3254, 2010.

[6] Gilles Aubert and Pierre Kornprobst, *Mathematical problems in image processing: partial differential equations and the calculus of variations*, vol. 147, Springer Science & Business Media, 2006.

[7] Kien Nguyen, Anindya Sarkar, and Anil K Jain, "Structure and context in prostatic gland segmentation and classification," in *International Conference on Medical Image Computing and Computer-Assisted Intervention*. Springer, 2012, pp. 115–123.

[8] Andrew Janowczyk and Anant Madabhushi, "Deep learning for digital pathology image analysis: A comprehensive tutorial with selected use cases," *Journal of pathology informatics*, vol. 7, 2016.